

Feasibility of Interstage Cooling for a Geothermal sCO₂ Power Plant

Owen M. Pryor, Ph.D.
Senior Research Engineer
Southwest Research Institute
San Antonio, Texas

Reese W. Roddy
Engineer
Southwest Research Institute
San Antonio, Texas

Lev Ring, Ph.D.
President
Sage Geosystems
Houston, Texas

Doug Simpkins
Director of Simulation
Sage Geosystems
Houston, Texas

Victoria McGuire
Engineering Intern
Sage Geosystems
Houston, Texas



Dr. Owen Pryor is a Senior Research Engineer at Southwest Research Institute focusing on thermodynamics, cycle design, energy storage, carbon capture and advanced power cycles. Dr. Pryor has worked on sCO₂ related technologies for over 10 years, starting with fundamental experiments on sCO₂ oxy-combustion chemical kinetics during his Ph.D. at the University of Central Florida to component and system design for diverse sCO₂ applications. Dr. Pryor holds three patents, with two more pending, in the energy technology field.



Mr. Reese Roddy is an Engineer in the Rotating Machinery Development Section at Southwest Research Institute® (SwRI®). His work focuses on instrumentation and controls, off-design turbomachinery analysis, and thermal-fluid cycle modeling for geothermal power technologies and organic Rankine cycles (ORCs). He has also performed techno-economic analyses for turbomachinery and sCO₂ power cycle applications. Mr. Roddy earned his B.S. in Mechanical Engineering, Summa Cum Laude, from the University of Texas at San Antonio in 2023.



Dr. Lev Ring is President & Co-founder of Sage Geosystems with over 25 years in the oil and gas industry, managing engineering and R&D teams in drilling and well construction. His most recent role was the Director of Technology Development at Weatherford, where he commercialized Managed Pressure Drilling (MPD) technology into a \$500 million annual revenue business. Before joining Weatherford, Lev was the CTO and co-founder of Enventure Global Technologies, a joint venture between Shell and Halliburton. Lev holds more than 120 patents in the areas of drilling, well construction, well completion, next-generation geothermal, and energy storage. He has a PhD degree in Physics from the Russian Academy of Sciences, and an MS from the Moscow Institute of Physics and Technology.



Douglas Simpkins is Director of Simulation and Modeling at Sage Geosystems where he leads development of mathematical models, simulations, and engineering software for predicting behavior of geothermal processes. His team's work has focused on the development of tools, which incorporate surface, wellbore and subsurface models integrated into a common system level platform.



Victoria McGuire is a Mechanical Engineering Intern at Sage Geosystems developing thermodynamic models power cycles to support equipment decisions for 1-30+ MW geothermal and energy storage systems.

ABSTRACT

Supercritical carbon dioxide (sCO₂) power cycles have been studied for a wide range of energy applications, including oxy-combustion, waste heat recovery, energy storage, and geothermal power production. This work examines the impact of interstage cooling on a low-temperature geothermal sCO₂ system with a 200 °C heat source. Two cycle architectures were analyzed: (1) a simple non-recuperated cycle, and (2) a simple recuperated cycle. For each configuration, one or two stages of intercooling were considered to assess impacts on net power output and economic viability. Results show that introducing a single intercooling stage increased net power output by approximately 5%, while two stages yielded an improvement of about 9% compared to the baseline. These performance gains were achieved with minimal changes to overall capital cost; however, cooling system performance itself had a significant effect, with potential variations in cost on the order of 10–20%. Based on the combined performance and economic results, a single stage of intercooling appears to offer the most practical balance, delivering a meaningful efficiency gain without increasing capital costs, while also improving operational flexibility in geothermal sCO₂ cycles.

INTRODUCTION

The U.S. is projected to increase its electricity consumption by 30-40% over the next two decades according to the EIA [1]. In order to meet this demand renewable energy is expected to increase by over 400% in that time span. To meet this rising demand, technologies such as geothermal power need to increase dramatically.

Current geothermal power plants often operate for 20 or 30 years and are expected to provide constant reliable renewable energy but require specific site conditions to make the projects economically feasible. These systems often require easily accessible hot-water such as the Beowawe Plant in Nevada [2] or steam such as The Geysers in California [3]. Recent advances in new power cycles (such as supercritical carbon dioxide, sCO₂) and drilling techniques have allowed for the performance potential of geothermal power plants over a much wider subsurface and geographical range than the current state-of-the-art geothermal power plants. The most common type of novel cycle is the ORC power cycle utilizing common fluids such as R-134a, R-600, R-600a, etc. [4]. The problem is struggle with the large temperature variations between the initial well conditions and the final temperatures at the end of the well life, as well as elevated

ambient temperatures resulting in significant reductions in the power output. To overcome these limitations, alternative working fluids and cycle architecture are being investigated.

Supercritical carbon dioxide is another working fluid that has been explored for geothermal systems that may be able to mitigate some of these concerns [8]. This paper investigates the addition of inter-stage cooling on the impact of a geothermal power cycle in terms of both cost and performance of the cycle. Cost correlations were taken from the literature for the capital costs of the cycle.

MODEL DESCRIPTION

The system was modeled using NPSS [1] in conjunction with thermodynamic properties from NIST Standard Reference Database 23 (REFPROP) [12]. Previous works have shown that NPSS is able to accurately model sCO₂ power cycles, energy storage systems and other cycles accurately for closed cycle models [13]. Preliminary analysis indicated that its performance gains were marginal compared to the recuperated cycle, and it added complexity without clear economic advantage. This work focused on a model with five main process components to extract power from a geothermal reservoir over time as shown in Figure 1.

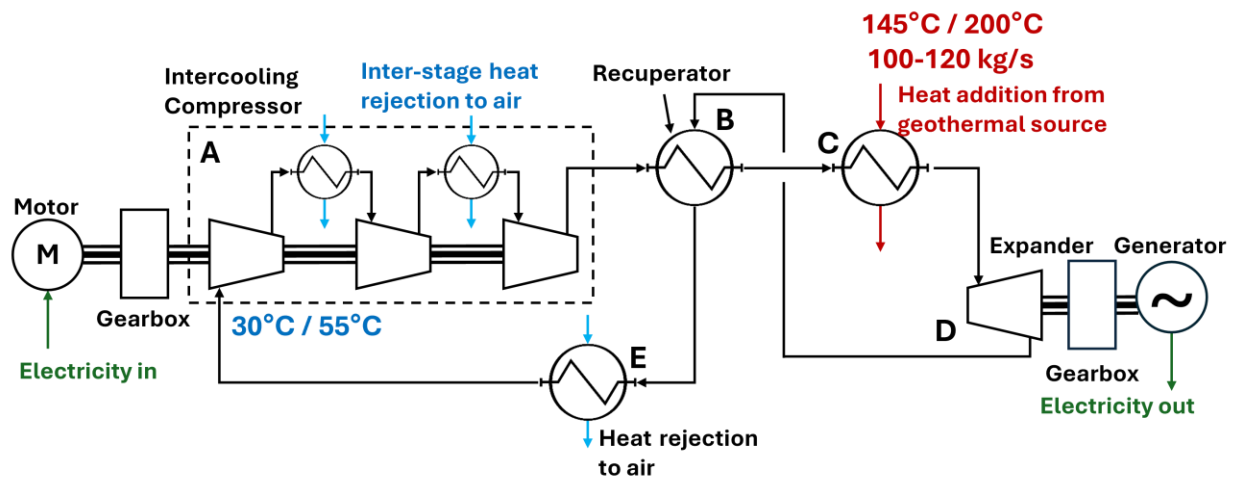


Figure 1. Process Flow Diagram of the Geothermal Cycle Model

The intercooled compressor (A) was modeled using a series of simple compressors with a counterflow heat exchanger between each consecutive compressor stages with air as the secondary fluid. The recuperator (B) and the primary heater (C) were modeled as a single counter-flow heat exchanger each. The primary heater used water as the secondary fluid inside the heat exchanger. The turbine (D) was modeled as a single expansion stage with a fixed efficiency at the design point. The process cooler (E) was modeled as a counterflow heat exchanger with air as the secondary fluid. Additional components including the gearboxes, motor, generator and the fan power for the process cooler were included in the model. Table 1 shows the main assumptions of the model for the various components. The number of stages for the compressor varied between 1-3 stages for all simulations.

Table 1. Key Component Assumptions for Cycle Model

Parameter	Value
Geothermal Source Mass Flow	100 kg/s

Parameter	Value
Compressor Isentropic Efficiency	84%
Turbine Isentropic Efficiency	92%
Primary Heater Approach Temperature	10°C
Recuperator Minimum Approach Temperature	5°C
Process Cooler Approach Temperature	5°C
Intercooler Approach Temperature	5°C
Motor Efficiency	95%
Generator Efficiency	95%
Gearbox Efficiency	98%
Dry Cooler COP	70

The process conditions were varied for all cycle configurations. The sCO₂ flow rate varied between 150-250 kg/s while the turbine inlet pressure varied between 120-250 bar. The compressor inlet pressure was held constant at 80 bar for all simulations. An example of the parameterized cycle sweeps can be seen in Figure 2. On the left, the mass flow is shown on the x-axis while the pressure variation is displayed using the color scale (blue is lower pressures, red is higher pressures). The right figure shows the turbine inlet pressure on the x-axis, and the mass flow rate is shown via the color scale (blue is low mass flow rates, red is high mass flow rates).

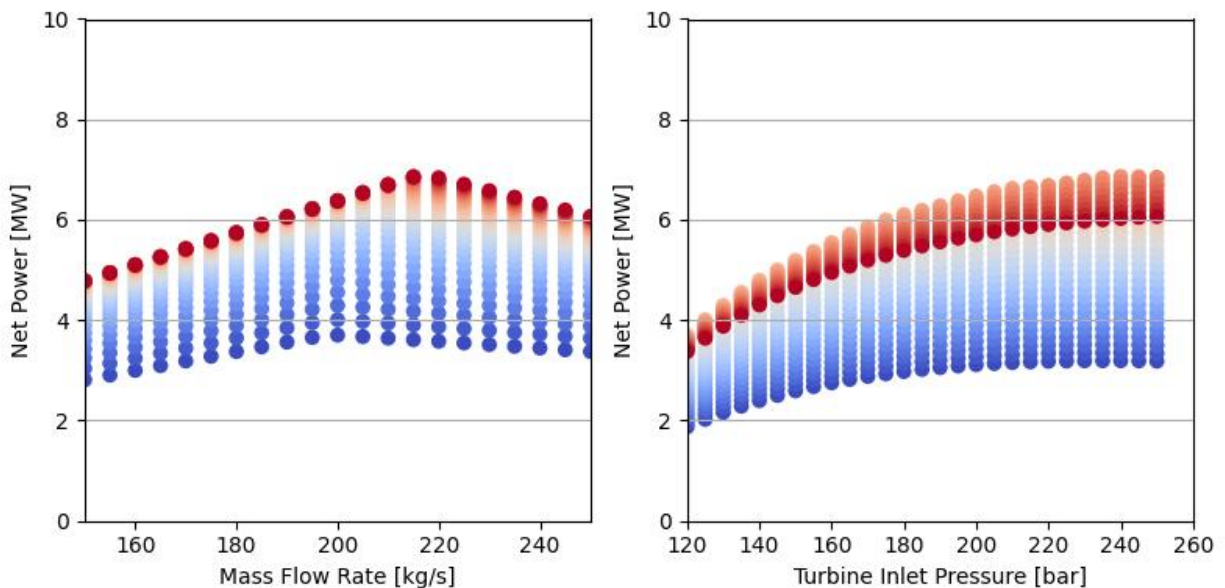


Figure 2. Example of Gross Shaft Power Parameterized Sweeps

Geothermal cycles have large variations in their boundary conditions over the course of the cycle. Four different sets of boundary conditions were modeled to represent the range of

geothermal source temperatures and boundary conditions. These four conditions represent the expected operating range over a 20-30 year well lifetime, with 200°C representing initial conditions and 145°C representing expected thermal degradation. Table 2 shows the boundary conditions below.

Table 2. Geothermal Boundary Conditions

Case Number	Case	Ambient Temperature	Source Temperature
1	Design Point	25°C	200°C
2	High Ambient Temperatures	50°C	200°C
3	Low Heat Source Temperature	25°C	145°C
4	Worst Conditions	50°C	145°C

The costs for the cycle were modeled from Weiland et al. [16]. The specific costs for each component can be found in Table 3. Each component was scaled from these equations based on the results from the cycle model. It should be noted that the Weiland Correlations were originally for a natural gas oxy-fuel sCO₂ cycle which is significantly hotter than the temperatures found in a geothermal cycle. As such, the geothermal cycle costs would most likely be conservative due to the lower temperatures. The compressor was modeled as a single body with multiple stages. The intercoolers were modeled as individual heat exchangers due to the pressure difference between each stage exit.

Table 3. Cost correlations for major components.
Specific cost correlations were taken from Weiland et al. [16].

Component	Unit	Equation	Weiland Component
Compressor	MWsh	$C = 1,230,000 \cdot P^{0.3992}$	Radial IG Compressor
Turbine	MWsh	$C = 406,200 \cdot P^{0.8}$	Radial Turbine
Primary Heater	MWth	$C = 632,900 \cdot Q^{0.60}$	Recuperator
Recuperator	W/K	$C = 49.45 \cdot UA^{0.7544}$	Recuperator
Process Cooler	W/K	$C = 32.88 \cdot UA^{0.75}$	Direct Air Cooler
Intercooler	W/K	$C = 32.88 \cdot UA^{0.75}$	Direct Air Cooler
Generator	MWe	$C = 108,900 \cdot P^{0.5463}$	Generator
Motor	MWe	$C = 399,400 \cdot P^{0.6062}$	Motor
Gearbox	MWsh	$C = 177,200 \cdot P^{0.2434}$	Gearbox

RESULTS AND DISCUSSION

Different trade studies were undertaken to understand the costs and performance of the cycle. The first trade study was to understand the impact of the different boundary conditions (Table 2) on the ability of the system to produce power. The design point is able to produce over 6 MW of net power regardless of the number of stages for the compressor at a compressor inlet temperature of 30 °C. Figure 3 shows the gross shaft power for the different boundary conditions and Figure 4 shows the net power. The sCO₂ at the inlet is considered a supercritical liquid and therefore does not have a significant temperature increase from the compressor which leads to

the interstage cooling having only a small impact on the results. When the ambient temperature is significantly higher, the power is significantly reduced due to the elevated compression power needed for the system. The interstage cooling is also shown to have a slightly negative impact at elevated ambient conditions on the power output as the stage count increases due to the high temperatures out of the compressor also allowing for a slightly higher flow rate of CO₂ for all of the results. The lower heat source temperature had a major impact on the results for the recuperated cycle. With only a single stage, the lower heat source results in the recuperator pinching the allowable expansion from 135C. With the addition of more stages and the lower compressor outlet temperature, the system is able to produce almost 3MW of gross shaft power and around 2.5 MW of electric power. The combination of the low heat source and elevated ambient conditions resulted in the two-stage compressor barely having positive shaft power and the three-stage system being less than 500 kW. Adding in the losses from the motor, gearbox, generator and the dry air cooler, none of the systems were able to produce positive net power.

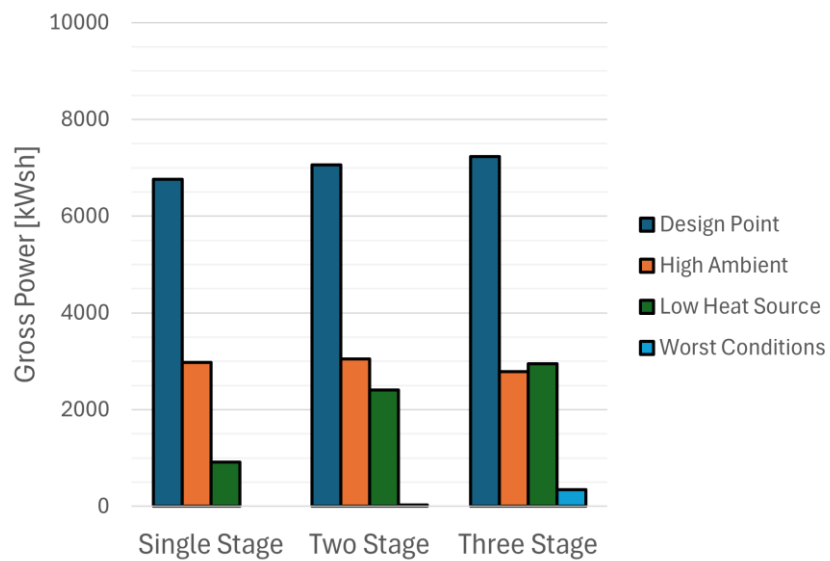


Figure 3. Comparison of the gross shaft power for three different compressor stage counts at different cycle conditions for a system without a recuperator.

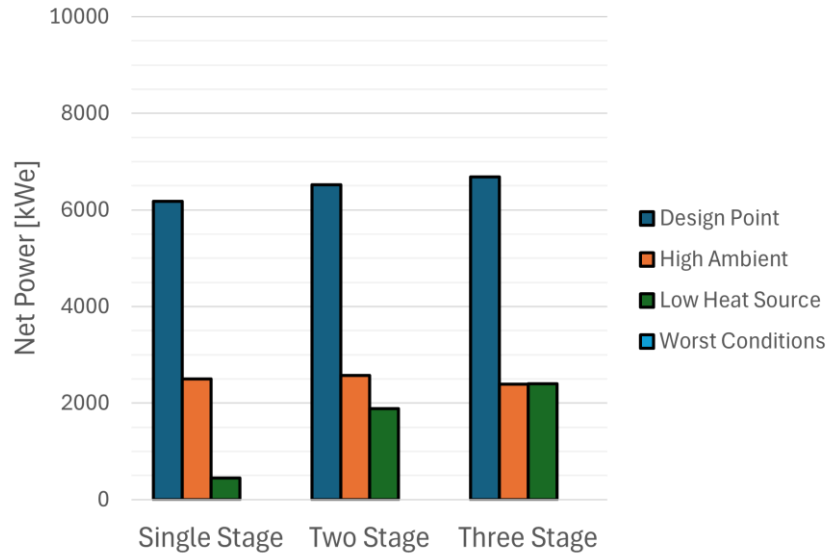


Figure 4. Comparison of the net power for three different compressor stage counts at different cycle conditions for a system without a recuperator.

For the remaining sweeps, two different cycle points were analyzed to understand the power output and costs of the surface equipment. The first point was the maximum net power output of the cycle sweeps after all parasitic losses were accounted for. The second point was the minimum specific capital costs of the entire system. The minimum specific capital costs were calculated by dividing the net power output of the cycle by the total capital costs based on the equations from Table 3. Figure 5 shows the maximum power output at the design point while Figure 6 shows the net power output at the minimum specific capital costs. Minimizing the specific costs resulted in a drop of around 1500 kW from the maximum gross shaft power and a 1000 kW from the net power output. Comparing end-of-life conditions, intercooled compression produces approximately 4-5 times more power than single-stage compression.

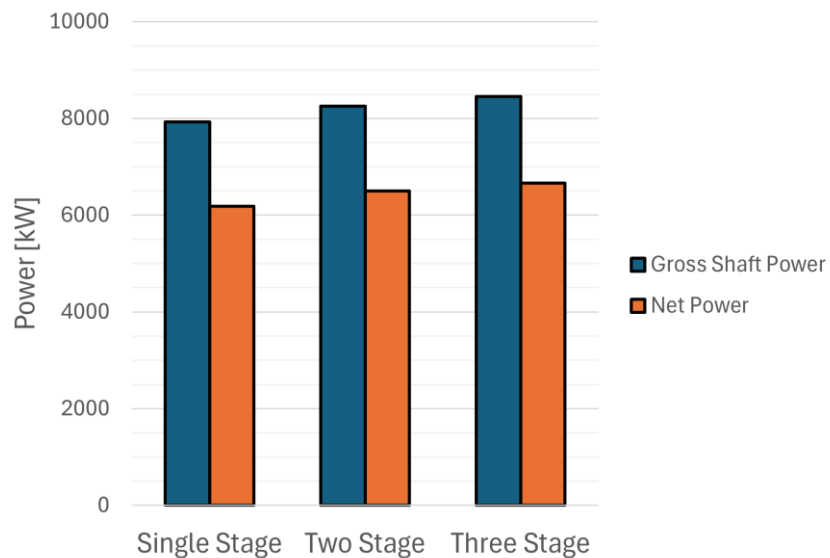


Figure 5. Comparison of the gross shaft power to the net power for a system that maximizes the net power output at the design point

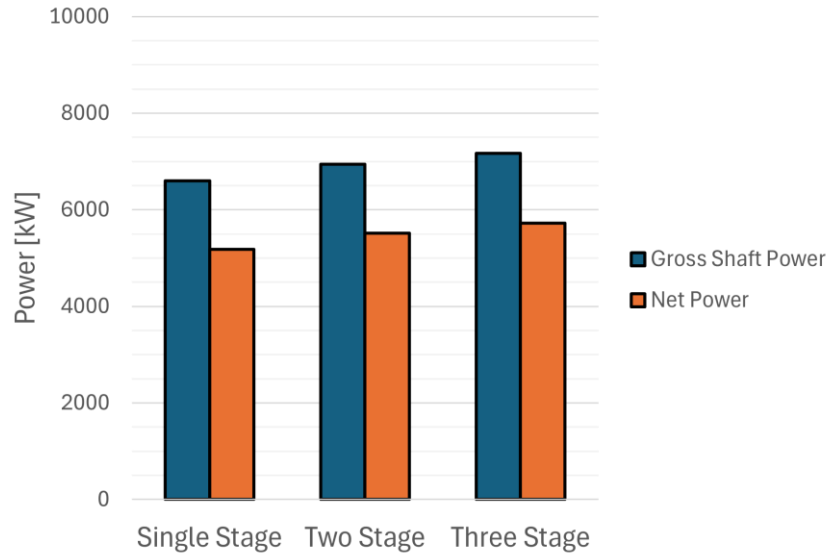


Figure 6. Comparison of the gross shaft power to the net power for a system that minimizes specific capital costs at the design point

The next trade study that was explored was the elimination of the recuperator from the cycle. As noted previously, the recuperator can become a detriment to the cycle as the ambient temperatures or the source temperature change. The impact on the net power was relatively small as shown in Figure 7. Removing the recuperator resulted in a loss of 500 kW for the intercooled systems while having almost no impact on the cycle without intercooling. For the non-intercooled system, the temperature difference between the high- and low-pressure sides of the heat exchanger become very small resulting on little heat being transferred from the fluid after expansion. The addition of intercooling allows for a slight increase in the power output of the cycle but not enough to justify the addition of an extra component to the costs.

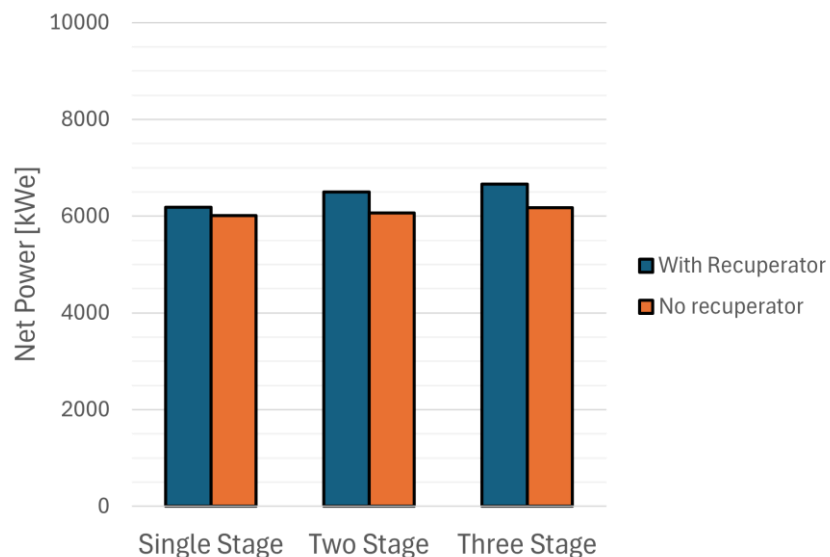


Figure 7. Impact of the recuperator on the net power output while maximizing the net power output at the design point of the system.

When minimizing the costs, the recuperator adds around 700 kW to the net power output of the cycle for all three configurations as shown in Figure 8.

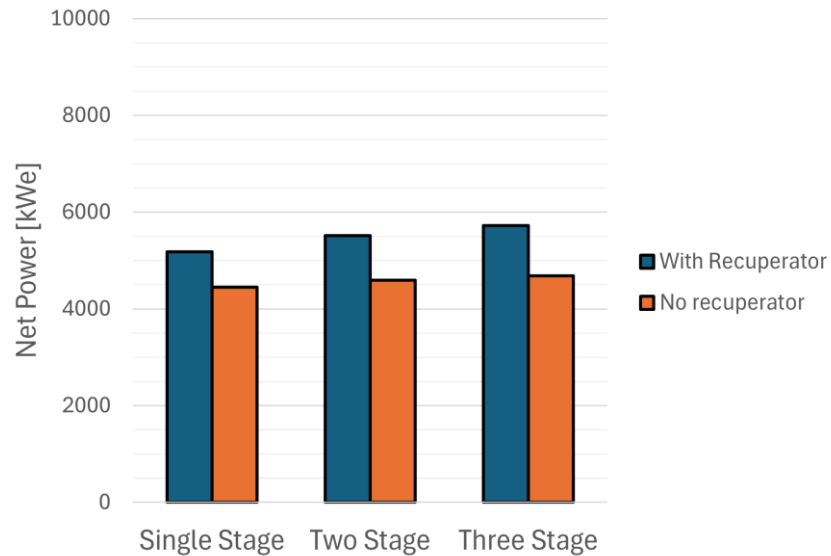


Figure 8. Impact of the recuperator on the net power output while minimizing the specific capital costs at the design point of the system.

The specific capital costs of each component are shown in Figure 9 when the system is designed to maximize the power output and Figure 10 for the minimal specific costs of the system. When maximizing the net power, the specific costs of the system decrease initially when adding intercooling to the system. This result is from the reduction in the primary heater needed for the cycle and the recuperator increasing the heat recovered from the expanded process. The heater decreases from a specific cost of \$1500/kWe to less than \$1000/kWe at the cost of additional cooling. Since the intercoolers are modeled as individual heat exchangers, the costs increase with the additional cooling outstrip the heater cost reductions for the three-stage compressor. The minimal costs show that a single compression stage is ideal while the costs increase by around \$500/kWe for a three-stage compressor.

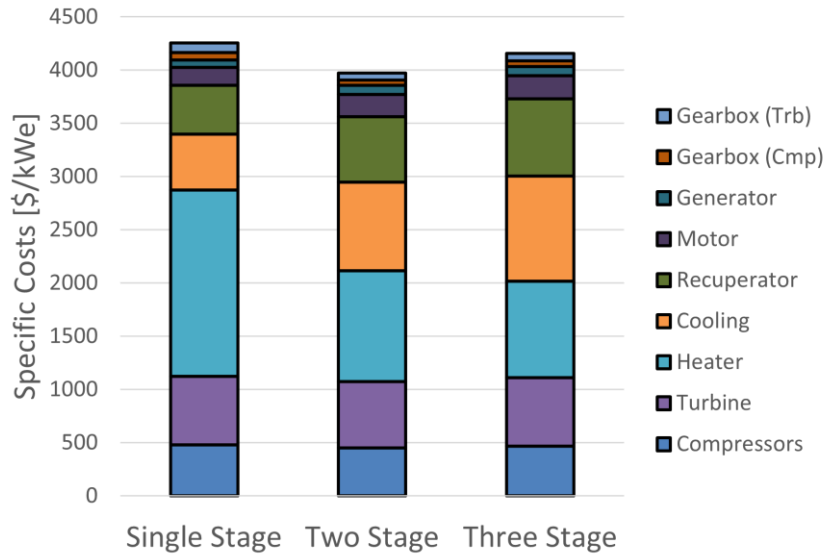


Figure 9. Specific capital costs for the system while maximizing the net power output of the cycle.

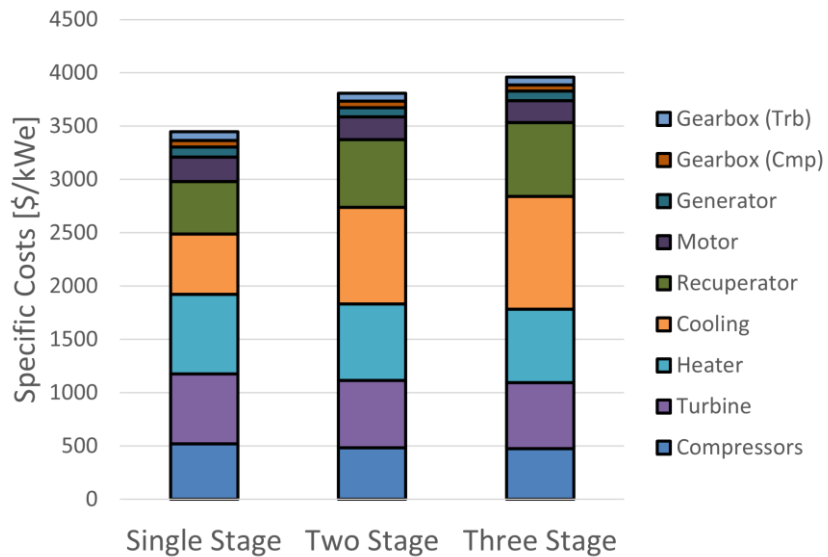


Figure 10. Minimum specific capital costs at the design point.

Adding the recuperator to the cycle was shown to result in around \$400/kWe increase in the costs despite the significant increase in the power output of the cycle as shown in Figure 11 and Figure 12. The three main heat exchangers in the system are the cost, a combined \$1700-2500 per kWe with the recuperator in place for the minimum cost cases but are reduced to \$1200-\$1600 without the recuperator.

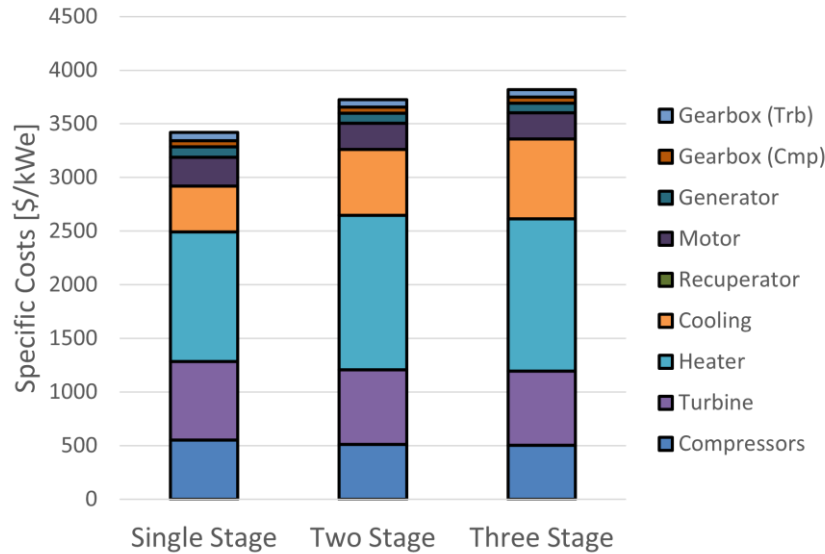


Figure 11. Specific capital costs for the system while maximizing the net power output for cycle without the recuperator.

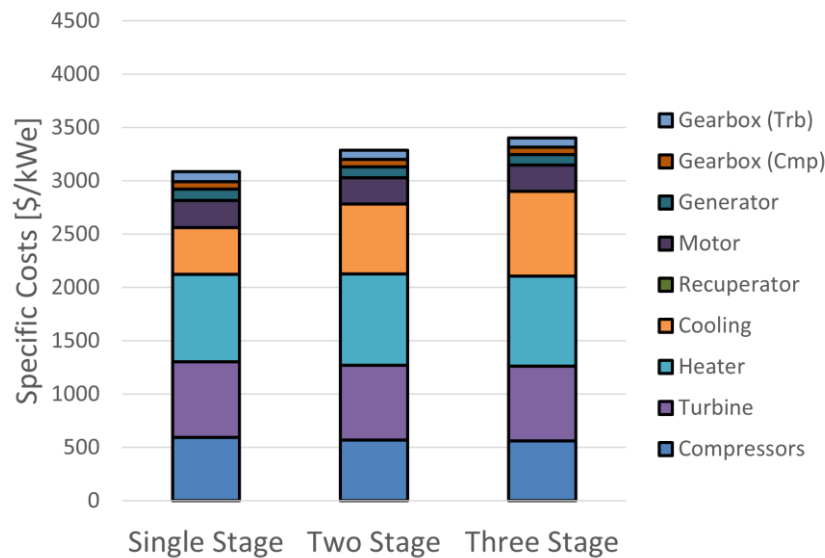


Figure 12. Minimum specific capital costs for the system for cycle without the recuperator.

CONCLUSIONS

A single stage of intercooling offers the best balance of efficiency, cost, and operational flexibility. Inter-stage cooling has the potential to improve the performance of geothermal power cycles and help minimize the fall-off in power production that results from the lower temperature outputs near the end of the cycle. With the addition of one stage with intercooling between the stage, the design point only had a slight increase in power production but by the end of the lifespan of the well, it is assumed that the system could extract four times the amount of power from the same source. Additionally, the recuperator, often a necessary component for sCO₂ power cycles, was able to be removed, which had a moderate impact on the performance of the cycle. Cost

estimates were made based on correlations from the literature which show that costs for the system are 10 to 20% higher with the addition of one or two stages compared to the results. Future work aims to refine the costs of the sCO₂ cycle for geothermal applications and determine if there is a feasible pathway to inter-stage cooling between compressor stages.

REFERENCES

- [1] U.S. Energy Information Administration. (2025). “*Annual Energy Outlook 2025*” (Release date: April 15 2025). U.S. Department of Energy.
- [2] ORMAT, 2022, “Beowawe 2022 RETA Application”.
- [3] Calpine Corporation, “About Geothermal Energy: The Geysers”. <https://geysers.com/geothermal>. Accessed on 12/27/23.
- [4] Zare, V., 2015, “A comparative exergoeconomic analysis of different ORC configurations for binary geothermal power cycles”, *Energy Conversion and Management* 105 (2015) 127-138.
- [5] Ahmadi, A., El Haj Assad, M., Jamali, D.H., Kumar, R., Li, Z.X., Salameh, T., Al-Shabi, M., Ehyaei, M.A., 2020, “Applications of geothermal organic Rankine Cycle for electricity production” *Journal of Cleaner Production*
- [6] Guo, T., Wang, H.X., Zhang, S.J., 2011, “Selection of working fluid for a novel low-temperature geothermally-powered ORC based cogeneration system”, *Energy Conversion and Management* 52 (2011) 2384-2391.
- [7] Yin, H., Sabau, A.S., Conklin, J.C., McFarlane, J., Qualls, A.L., 2013, “Mixtures of SF₆-CO₂ as working fluids for geothermal power plants”, *Applied Energy* 106 (2013) 243-253.
- [8] Brown, D. W., 2000, “A hot dry rock geothermal energy concept utilizing supercritical CO₂ instead of water”. In *Proceedings of the twenty-fifth workshop on geothermal reservoir engineering*, Stanford University (pp. 233-238).
- [9] Pruess, K. (2006). Enhanced geothermal systems (EGS) using CO₂ as working fluid—A novel approach for generating renewable energy with simultaneous sequestration of carbon. *Geothermics*, 35(4), 351-367.
- [10] Pan, L., Freifeld, B., Doughty, C., Zakem, S., Sheu, M., Cutright, B., & Terrall, T. (2015). Fully coupled wellbore-reservoir modeling of geothermal heat extraction using CO₂ as the working fluid. *Geothermics*, 53, 100-113.
- [11] Claus, R. W., Evans, A. L., Lylte, J. K., & Nichols, L. D. (1991). Numerical propulsion system simulation. *Computing Systems in Engineering*, 2(4), 357-364.
- [12] Lemmon, E. W., Bell, I. H., Huber, M. L., & McLinden, M. O. (2018). NIST standard reference database 23: reference fluid thermodynamic and transport properties-REFPROP, Version 10.0, National Institute of Standards and Technology. *Standard Reference Data Program, Gaithersburg*.
- [13] Smith, N. R., Tom, B., Rimpel, A., Just, J., Marshall, M., Khawly, G., ... & Hoopes, K.

(2022, June). The Design of a Small-Scale Pumped Heat Energy Storage System for the Demonstration of Controls and Operability. In Turbo Expo: Power for Land, Sea, and Air (Vol. 86014, p. V004T07A012). American Society of Mechanical Engineers.

- [14] Tom, B., Smith, N., & McClung, A. (2020, September). Cycle Considerations for the Conceptual Design of a Pumped Heat Energy Storage System. In Turbo Expo: Power for Land, Sea, and Air (Vol. 84140, p. V005T07A005). American Society of Mechanical Engineers.
- [15] Katcher, K., Marshall, M., Smith, N.R., Replogle, C. (2021). "Estimated Cost and Performance of a Novel sCO₂ Natural Convection Cycle for Low-grade Waste Heat Recovery", Proceedings of the 4th European Conference for Energy Systems, March 23-24, 2021, Online.
- [16] Weiland, N., White, C. (2019). "Performance and Cost Assessment of a Natural Gas-Fueled Direct sCO₂ Power Plant," NETL-PUB-22274, National Energy Technology Laboratory, U.S. Dept. of Energy, March 15, 2019.